PHYSICAL REVIEW D **72,** 015007 (2005)

Diquark and pion condensation in random matrix models for two-color QCD

B. Klein
Institute for Theoretical Physics, University of Heidelberg, Philosophenweg 19, 69120 Heidelberg, Germany

D. Toublan
Department of Physics, University of Illinois at Urbana-Champaign, Urbana, Illinois 61801-3080, USA

J. J. M. Verbaarschot
Department of Physics and Astronomy, State University of New York at Stony Brook, Stony Brook, New York 11794-3800, USA
(Received 29 March 2005; published 18 July 2005)

We introduce a random matrix model with the symmetries of QCD with two colors at nonzero isospin and baryon chemical potentials and temperature. We analyze its phase diagram and find phases with condensation of pion and diquark states in addition to the phases with spontaneously broken chiral symmetries. In the limit of small chemical potentials and quark masses, we reproduce the mean field results obtained from chiral Lagrangians. As in the case of QCD with three colors, the presence of two chemical potentials breaks the flavor symmetry and leads to phases that are characterized by different behaviors of the chiral condensates for each flavor. In particular, the phase diagram we obtain is similar to QCD with three colors and three flavors of quarks of equal masses at zero baryon chemical potential and nonzero isospin and strange chemical potentials. A tricritical point of the superfluid transitions found in lattice calculations and from an analysis in terms of chiral Lagrangians does not appear in the random matrix model. Remarkably, at fixed isospin chemical potential, for the regions outside of the superfluid phases, the phase diagrams in the temperature—baryon chemical potential plane for two colors and three colors are qualitatively the same.

DOI: 10.1103/PhysRevD.72.015007 PACS numbers: 12.38.Aw, 11.30.Rd

I. INTRODUCTION

Recently, the phase diagram of QCD at nonzero chemical potential for the baryon number has received a great deal of attention. It has been found that a plethora of phase transitions are possible as a function of the baryon chemical potential, μ_B, the isospin chemical potential, μ_I, and the temperature T. Among others, a superconducting phase [1,2], a pion condensate [3,4] and a critical endpoint have been predicted [1,5,6] (see [7] for a review). A systematic analysis of the phase diagram is possible in the $\mu_B = 0$ plane and, perturbatively, for asymptotically large values of μ_B [8]. At finite, not asymptotically large baryon chemical potential, where the interactions between the quasiparticles that carry color charge are strong, the theoretical basis of these predictions is rather weak. So far, it has not been possible to confirm the existence of the proposed phases in this region, neither from experimental results nor from lattice calculations. The reason for the failure of standard lattice simulations is that in the presence of a chemical potential for baryons the fermion determinant in the partition function becomes complex so that a probabilistic interpretation of the partition function is not possible.

Thus, it is attractive to try to gain insight into the properties of such condensed phases by studying QCD-like theories which avoid some of these complications. In this paper we study QCD with two colors with baryons that are colorless diquark states. As in the case of three colors, chiral symmetry is spontaneously broken and the theory is confining at low temperatures and chemical potential. However, at nonzero baryon number chemical potential, two important simplifications occur in this theory. First, the condensing diquark states are Goldstone bosons associated with the spontaneous breaking of chiral symmetry with a critical chemical potential equal to half the pion mass. This makes it possible to analyze the condensed phase by means of chiral Lagrangians [9–13]. Second, as a consequence of the pseudoreality of the SU(2) gauge group, the fermion determinant remains real when a chemical potential is introduced. Therefore, for an even number of flavors, this theory can be simulated on the lattice without encountering a sign problem.

The phase diagram in two-color QCD has been studied using a variety of methods. The appearance of a baryonic diquark condensate above a critical chemical potential of $\mu_{Bc} \simeq m_\pi/2$ was first observed in lattice simulations at strong coupling [14–16]. More recently, the phase diagram was analyzed in the framework of chiral Lagrangians [9–12], where it was found that the critical value of the chemical potential is indeed given by the mass of the lightest state, and that the transition is of second order at zero temperature. Lattice simulations confirm these results [17–32]. In [26,29,30] it was observed that beyond a critical value of the baryon chemical potential and temperature, the transition to the diquark condensation transition ceases to be of second order and becomes a first order transition. This implies the existence of a tricritical point. In chiral perturbation theory, such a tricritical point was found [11,33] at values for the chemical potential and the temperature of the order of the pion mass m_π.

In physical applications, such as in neutron stars or in heavy ion collisions, the chemical potentials for different quark flavors are not necessarily equal. While the chemical potential for baryon charge is the same for all quarks, an additional isospin chemical potential parameterizes the difference between the chemical potentials for two light quark flavors. Its effect on the phase diagram has been studied for $N_c = 2$ in [13] using effective chiral Lagrangians, and for $N_c = 3$ in [34] using a random matrix model, in [35–37] by means of a Nambu–Jona-Lasinio model, and in [38] within the ladder approximation.

In this article, we employ a random matrix model to study QCD with two colors at finite chemical potentials for isospin and baryon density and finite temperature. Originally, random matrix models have been introduced in QCD in order to describe correlations of low-lying eigenvalues of the Dirac operator [39,40]. These random matrix models are equivalent to the static part of a chiral Lagrangian which is uniquely determined by the symmetries of the microscopic theory [41–44]. From this connection, it has been shown that they provide an exact analytical description of correlations in the low-lying Dirac spectrum. In addition to their use as exact analytical models for the spectrum, random matrix models can also serve as schematic models for the phase transitions in QCD. The first of these models was introduced in [45,46] to describe the chiral restoration transition at finite temperature. At finite baryon chemical potential, they have been successfully used to explain the failure of the quenched approximation in lattice QCD [47], and to predict a tricritical point for the chiral restoration transition at finite density and temperature [6]. The static part of the effective chiral Lagrangian for QCD with the coupling of charged Goldstone bosons to a chemical potential has also been derived from a chiral random matrix model [48]. More recently, closely related models with a random gauge potential have been considered for the superconducting phases [49,50] and for diquark condensation for $N_c = 2$ [51]. Though these models have additional symmetries beyond those considered in this article, they lead to the same spectral density as the corresponding chiral random matrix ensembles [52].

The random matrix theory approach rests on the idea that it is the matrix equivalent of a Landau-Ginzburg potential. Both theories are based on the symmetries of the microscopic partition function. Indeed, as we will also see in this paper, it is possible to derive a Landau-Ginzburg functional from the random matrix theory. The presence of a diquark and a pion condensation phase raises several interesting questions, which can be addressed by studying a random matrix model. In particular, we hope to investigate the robustness of the tricritical point that has been found in lattice simulations [30] and in chiral perturbation theory [11]. In general, we wish to identify which features of the phase diagram are generic and due to the underlying symmetries and which features are model dependent.

This article is organized as follows. In Sec. II, we give a short review of the symmetries and phase diagram of the partition function of QCD with two colors. Our random matrix model is introduced in Sec. III. We show that it can be rewritten exactly in terms of the static part of a chiral Lagrangian. With an ansatz based on the structure of the expected condensates we obtain an effective potential for these condensates. Our main results are presented in Sec. V, where we analyze the phase diagram in the μ_B–μ_I chemical potential plane. Concluding remarks are made in Sec. VI.

II. QCD WITH TWO COLORS

The partition function for QCD with two colors is given by

$$Z_{\rm QCD} = \left\langle \prod_{f=1}^{N_f} \det(D + m_f + \mu_f \gamma_0) \right\rangle, \qquad (2.1)$$

where the Euclidean Dirac operator is $D = \gamma_\mu D_\mu = \gamma_\mu(\partial_\mu + iA_\mu)$, γ_μ are the Euclidean γ-matrices, and A_μ is the SU(2)-valued gauge potential. For each of the N_f quark flavors, the quark mass is given by m_f and the chemical potential by μ_f. The brackets denote an average over the Euclidean Yang-Mills action. In the case of only two flavors, the chemical potentials can be expressed in terms of isospin and baryon chemical potential,

$$\mu_B = \frac{1}{2}(\mu_1 + \mu_2), \qquad \mu_I = \frac{1}{2}(\mu_1 - \mu_2). \qquad (2.2)$$

Because of the pseudoreality of the SU(2) gauge group, the flavor symmetry group is enlarged to SU($2N_f$) from the usual SU(N_f) $\times$ SU(N_f) in case of QCD with three or more colors. In the vacuum, this symmetry is spontaneously broken to Sp($2N_f$). Thus, in the chiral limit, one expects $N_f(2N_f - 1) - 1$ exactly massless Goldstone bosons. Among these Goldstone bosons there are diquark states which carry baryon charge, in addition to the mesonic pion states which carry a charge with respect to isospin number. The mass term breaks the chiral flavor symmetry explicitly down to Sp($2N_f$). A baryon chemical potential term by itself is invariant under an U(1)$_B$ $\times$ SU(N_f) $\times$ SU(N_f) subgroup of the original SU($2N_f$), and in the presence of a mass term this symmetry is further broken down to U(1)$_B$ $\times$ SU(N_f).

The presence of an additional chemical potential coupling to light bosonic states greatly increases the number of possible phases. At low temperature and chemical potential we expect that chiral symmetry is spontaneously broken. The phases with broken chiral symmetry are characterized by the order parameters $\langle \bar{u}u \rangle$ and $\langle \bar{d}d \rangle$. As in the case of $N_c = 3$ [34], in the presence of two different chemical potentials for the two flavors u and d, there is no reason to believe that $\langle \bar{u}u \rangle = \langle \bar{d}d \rangle$, and in general, one expects

that the chiral condensates for both flavors are not equal. At $\mu_I \neq 0$, when the two chemical potentials are different, it cannot be excluded that chiral symmetry restoration will take place via two separate phase transitions.

In addition to the pion condensate $\rho = \frac{1}{2} \times (\langle \bar{u}\gamma_5 d\rangle - \langle \bar{d}\gamma_5 u\rangle)$, already known from the case $N_c = 3$, which appears above a critical isospin chemical potential, for QCD with two colors we also have a diquark condensate $\frac{1}{4} i(\langle d^\dagger u^*\rangle - \langle u^\dagger d^*\rangle + \langle d^T u\rangle - \langle u^T d\rangle)$ above a critical baryon chemical potential. From general arguments, one expects a phase transition when the chemical potential becomes equal to the ratio of the mass and the charge for the lightest charged excitation. Indeed, this has been shown explicitly by an analysis in terms of chiral Lagrangians at low chemical potential and temperature [9–13]. It was also found that the transition to a baryonic diquark condensation phase or a pion condensation is of second order.

From the symmetries of the partition function alone, it is possible to predict some of the properties of the phase diagram. As has been shown in [9,10], the determinantal term in the partition function (2.1) can be rewritten in such a way that the enlarged flavor symmetry becomes manifest. Using a chiral representation for the Euclidean γ-matrices, in which $\gamma_0\gamma_\mu = \mathrm{diag}(i\sigma_\mu, -i\sigma_\mu^\dagger)$ with the spin matrices $\sigma_\mu = (-i, \sigma_k)$, and the pseudoreality property of the generators of the gauge group, $-\tau_2\tau_a\tau_2 = \tau_a^*$, the fermionic part of the Lagrangian with the Dirac operator can be rewritten in terms of a new spinor basis. In the chiral limit $m_f \to 0$, but including a nonzero chemical potential, it becomes

$$\begin{pmatrix} \psi_L^* \\ \tilde{\psi}_R^* \end{pmatrix}^T \begin{pmatrix} i\sigma_\mu D_\mu + \mu_f & 0 \\ 0 & i\sigma_\mu D_\mu - \mu_f \end{pmatrix} \begin{pmatrix} \psi_L \\ \tilde{\psi}_R \end{pmatrix}, \quad (2.3)$$

where the spinors $\tilde{\psi}_R = \sigma_2\tau_2\psi_R^*$ transform in the same representation of the color group as the spinors ψ_L. Clearly, at $\mu_f = 0$ and $m_f = 0$, the flavor symmetry group is enlarged to SU($2N_f$). For two flavors, the fermion determinant in the partition function factorizes into

$$\begin{aligned} &\det(m^2 - (iD_\mu\sigma_\mu + \mu_1)\sigma_2\tau_2(i(D_\mu\sigma_\mu)^T - \mu_1)\sigma_2\tau_2) \\ &\quad \times \det(m^2 - (iD_\mu\sigma_\mu + \mu_2) \\ &\quad \times \sigma_2\tau_2(i(D_\mu\sigma_\mu)^T - \mu_2)\sigma_2\tau_2). \end{aligned} \quad (2.4)$$

The partition function is therefore invariant under the interchanges $\mu_f \to -\mu_f$, $f = 1, 2$, and $\mu_1 \leftrightarrow \mu_2$. Translated into the physical chemical potentials, the partition function is invariant under the individual sign changes $\mu_I \to -\mu_I$ and $\mu_B \to -\mu_B$, and under the interchange $\mu_I \leftrightarrow \mu_B$. The latter symmetry, which amounts to $\mu_2 \to -\mu_2$, means the interchange of quarks and conjugate antiquarks. Under this transformation, a diquark condensate is transformed into a pion condensate. Thus, overall one expects that the phase diagram is symmetric about the lines $\mu_I^2 = \mu_B^2$ and the lines $\mu_I = 0$ and $\mu_B = 0$. Therefore from the symmetry of the QCD partition function we can restrict our study of the phase diagram to one half quadrant in the $\mu_B - \mu_I$-plane.

III. RANDOM MATRIX MODEL

We will introduce a random matrix model for QCD with two colors and study its phase diagram at finite chemical potentials for isospin and baryon number and finite temperature. The idea of the random matrix model is to replace the matrix elements of the Dirac operator by Gaussian distributed random variables, while respecting all the global symmetries of the QCD partition function. The dependence on temperature and chemical potentials will enter through external fields, which are also subject to symmetry constraints.

Besides the chiral and flavor symmetries, the Dirac operator can also have additional antiunitary symmetries. For an SU(2) gauge group, the Dirac operator satisfies the commutation relation

$$[iD, C\tau_2 K] = 0, \qquad (C\tau_2 K)^2 = 1, \quad (3.1)$$

where $C = \gamma_2\gamma_4$ is the charge conjugation matrix, τ_2 is a generator of the gauge group, and K is the complex conjugation operator. Because of this antiunitary symmetry, it is possible to find a basis in which all matrix elements of D are real. Thus, the matrices in the corresponding random matrix ensemble will have real entries, which is denoted by the Dyson index $\beta = 1$.

In the absence of a temperature and chemical potential, the matrix elements of the Dirac operator are simply replaced by real random variables with a Gaussian distribution. The chemical potential breaks the flavor symmetry in the same way as in the QCD partition function. Just as the dependence on the chemical potentials, an effective temperature dependence enters through an external field [45]. Because of the flavor symmetries and antiunitary symmetries of the partition function the temperature field has to satisfy the following conditions

(a) The temperature term must be real.
(b) It may not break the flavor symmetry.
(c) Its eigenvalues are given by $\pm inT$. In this article, we will consider only $n = 1$.

A real temperature term satisfying these constraints is given by the matrix

$$\omega(T) = \begin{pmatrix} 0 & T \\ -T & 0 \end{pmatrix}. \quad (3.2)$$

For vanishing chemical potential, such a temperature term leads to a second order phase transition [45]. We wish to stress that the temperature term here is different from the one for QCD with three colors.

The matrix representation for the Dirac operator in the random matrix model with two flavors is

$$D = \begin{pmatrix} m_1 & 0 & W+\omega(T)+\mu_1 & 0 \\ 0 & m_2 & 0 & W+\omega(T)+\mu_2 \\ -W^T-\omega(T)^T+\mu_1 & 0 & m_1 & 0 \\ 0 & -W^T-\omega(T)^T+\mu_2 & 0 & m_2 \end{pmatrix}, \tag{3.3}$$

where W is a real $n \times n$ matrix. The probability distribution of its matrix elements is given by

$$P(W) = \exp\Big[-\frac{n}{2}G^2 \mathrm{Tr} W^T W\Big]. \tag{3.4}$$

When we write the determinant as an integral over fermionic variables, the random matrix partition function becomes

$$Z_{\mathrm{RMT}} = \int \mathcal{D}W \prod_f d\psi^f d\bar{\psi}^f P(W) \exp[-\bar{\psi} D \psi]. \tag{3.5}$$

We will also include source terms for a pion condensate,

$$\lambda \frac{1}{2}\bar{\psi}\gamma_5 i\tau_2 \psi, \tag{3.6}$$

and for a diquark condensate,

$$j\frac{1}{4}(\psi^T \tau_2 \psi + \bar{\psi}^T \tau_2 \bar{\psi}), \tag{3.7}$$

where the antisymmetric Pauli matrix τ_2 acts in flavor space.

For a fixed number of flavors ($N_f = 2$), the partition function is a function of μ_1, μ_2, T and m_1, m_2, λ, j. While the masses act as source terms for the chiral condensates, they are also parameters of the model.

IV. EFFECTIVE PARTITION FUNCTION

Because of the unitary invariance of the random matrix partition function, it is possible to rewrite it in terms of effective degrees of freedom. We will do this below, and then analyze the resulting effective partition function, first to lowest order in chiral perturbation theory and then beyond this domain.

Starting from the random matrix partition function (3.5), we perform the Gaussian integrations over the elements of the random matrix. To decouple the resulting four-fermion terms, we perform a Hubbard- Stratonovich-transformation and introduce an integration over the mesonic low-energy degrees of freedom. The integrations over the fermionic variables can then be performed exactly. The resulting partition function in terms of the new variables is

$$Z^{\mathrm{eff}} = \int \mathcal{D}A \exp[-\mathcal{L}(A, A^\dagger)], \tag{4.1}$$

where

$$\mathcal{L} = \frac{n}{2}G^2 \mathrm{Tr} A A^\dagger - \frac{n}{4}\log\det Q'. \tag{4.2}$$

The dependence on the chemical potentials and the temperature is contained in the $8N_f \times 8N_f$ matrix Q'

$$Q' = \begin{pmatrix} A^\dagger + M & 0 & \mu_I I_3 + \mu_B B & -T \\ 0 & A^\dagger + M & T & \mu_I I_3 + \mu_B B \\ -(\mu_I I_3 + \mu_B B) & -T & A + M^\dagger & 0 \\ T & -(\mu_I I_3 + \mu_B B) & 0 & A + M^\dagger \end{pmatrix}. \tag{4.3}$$

The matrix A is a complex, antisymmetric $2N_f \times 2N_f$ matrix. All the source terms are contained in the $2N_f \times 2N_f$ matrix M, which for $N_f = 2$ is

$$M = \begin{pmatrix} 0 & m & -ij & \lambda \\ -m & 0 & \lambda & -ij \\ ij & -\lambda & 0 & m \\ -\lambda & ij & -m & 0 \end{pmatrix}. \tag{4.4}$$

where we have set $m_1 = m_2 = m$. From here on we will only consider quarks with equal mass. The chemical potentials enter as the coefficients of the matrices for baryon and isospin charges,

$$B = \mathrm{diag}(1, -1, 1, -1), \qquad I_3 = \mathrm{diag}(1, -1, -1, 1). \tag{4.5}$$

This particular form of the charge matrices is due to the appearance of quarks and conjugate antiquarks in the spinors transforming under the enlarged SU($2N_f$) symmetry, which have opposite charges with respect to the chemical potentials.

This effective Lagrangian can be simplified by a unitary transformation of the off-diagonal blocks, which leaves the value of the determinant unchanged. Exploiting the block structure, the effective Lagrangian (4.2) can be expressed as

$$\mathcal{L} = \frac{n}{2}G^2 \mathrm{Tr} A A^\dagger - \frac{n}{4}\log\det Q_+ Q_-, \tag{4.6}$$

where $Q_\pm$ are the $4N_f \times 4N_f$ matrices

$$Q_\pm = \begin{pmatrix} A^\dagger + M & \mu_B B + \mu_I I_3 \pm iT \\ -(\mu_B B + \mu_I I_3) \pm iT & A + M^\dagger \end{pmatrix}. \tag{4.7}$$

The effective partition function with Lagrangian (4.6) is invariant under

$$Q_\pm \to U Q_\pm U^T, \quad \mu_2 \to -\mu_2, \quad \lambda \to j, \quad j \to -\lambda, \tag{4.8}$$

with

$$U = \begin{pmatrix} 1 & & & \\ & i\sigma_1 & & \\ & & 1 & \\ & & & -i\sigma_1 \end{pmatrix}. \tag{4.9}$$

This transformation thus corresponds to an interchange of μ_B and μ_I and of the diquark condensate and the pion condensate.

We stress that this effective Lagrangian is an exact mapping of the original random matrix partition function.

A. Observables

We wish to study the partition function and obtain the phase diagram with regards to four order parameters: the chiral condensates $\langle \bar{u}u \rangle$ and $\langle \bar{d}d \rangle$ for the two quark flavors, the pion condensate $\frac{1}{2}(\langle \bar{u}\gamma_5 d \rangle - \langle \bar{d}\gamma_5 u \rangle)$ and the diquark condensate $\frac{1}{4} i(\langle d^\dagger u^* \rangle - \langle u^\dagger d^* \rangle + \langle d^T u \rangle - \langle u^T d \rangle)$. We identify these observables by taking the derivatives of the partition function with respect to the sources. After partial integration the expressions for the chiral condensates for the two flavors are given by

$$\begin{aligned} \langle \bar{u}u \rangle &= \frac{1}{2n} \partial_{m_1} \log Z^{\text{eff}} \\ &= G^2 \frac{1}{4} \langle A_{21} - A_{12} + A_{21}^* - A_{12}^* \rangle \equiv G^2 \sigma_1, \\ \langle \bar{d}d \rangle &= \frac{1}{2n} \partial_{m_2} \log Z^{\text{eff}} \\ &= G^2 \frac{1}{4} \langle A_{43} - A_{34} + A_{43}^* - A_{34}^* \rangle \equiv G^2 \sigma_2. \end{aligned} \tag{4.10}$$

For the pion condensate we find in terms of expectation values for the elements of the matrix A

$$\begin{aligned} \frac{1}{2}(\langle \bar{u}\gamma_5 d \rangle - \langle \bar{d}\gamma_5 u \rangle) &= \frac{1}{4n} \partial_\lambda \log Z^{\text{eff}}|_{\lambda=0} \\ &= G^2 \frac{1}{8} \langle A_{32} - A_{23} + A_{41} - A_{14} \\ &\quad + A_{32}^* - A_{23}^* + A_{41}^* - A_{14}^* \rangle \\ &\equiv G^2 \rho \end{aligned} \tag{4.11}$$

The diquark condensate is

$$\begin{aligned} &\frac{1}{4} i(\langle d^\dagger u^* \rangle - \langle u^\dagger d^* \rangle + \langle d^T u \rangle - \langle u^T d \rangle) \\ &\quad = \frac{1}{4n} \partial_j \log Z^{\text{eff}}|_{j=0} \\ &\quad = G^2 \frac{1}{8} i \langle A_{13} - A_{31} + A_{24} - A_{42} \\ &\qquad - A_{13}^* + A_{31}^* - A_{24}^* + A_{42}^* \rangle \\ &\quad \equiv G^2 \Delta. \end{aligned} \tag{4.12}$$

In our convention, expectation values of the diagonal blocks correspond to the chiral condensates, and expectation values of the off-diagonal blocks correspond to the diquark and pion condensates.

B. Chiral Lagrangian

The chiral Lagrangian is completely determined by the flavor symmetries of the microscopic theory and the pattern of the chiral symmetry breaking. Thus, it must be in agreement with the Lagrangian of chiral perturbation theory. For vanishing chemical potential and zero temperature, it has been shown that the random matrix partition function and the static part of the chiral Lagrangian in QCD are indeed equivalent [41–43].

To show this equivalence in the present case, we will expand the Lagrangian (4.6) in terms of the quark mass and the chemical potentials around the saddle point solution at $m = \mu_I = \mu_B = 0$. In accordance with the usual power counting rules [10] we use $m = \mathcal{O}(\epsilon^2)$ and $\mu_{I,B} = \mathcal{O}(\epsilon)$ and expand to second order in ϵ. In contrast to the case $N_c = 3$, the baryon chemical potential does not drop out of the effective Lagrangian. The baryon chemical potential couples to low-energy degrees of freedom in form of diquark states, which carry a baryon charge.

For vanishing mass and chemical potentials, the saddle point equation corresponding to (4.6) is given by

$$\frac{1}{G^2} A = (A^\dagger A + T^2) A, \tag{4.13}$$

which has the nontrivial solution

$$A = \frac{1}{G} \bar{\sigma}(T) \Sigma = \frac{1}{G} (1 - G^2 T^2)^{1/2} \Sigma, \tag{4.14}$$

where Σ is a complex, antisymmetric, unitary matrix. Expanding the effective Lagrangian (4.6) around this saddle point to order $\mathcal{O}(\epsilon^2)$, we find

$$\begin{aligned} \mathcal{L}(\Sigma) = \frac{n}{2} &(c_0(\mu_B, \mu_I, T) - G\bar{\sigma}(T) \text{Tr}(\Sigma M + \Sigma^\dagger M^\dagger) \\ &- G^2 \bar{\sigma}^2(T) \text{Tr}((\Sigma^\dagger(\mu_I I_3 + \mu_B B)\Sigma(\mu_I I_3 + \mu_B B)) \\ &+ \mathcal{O}(\epsilon^2)). \end{aligned} \tag{4.15}$$

We note that the temperature does not break any flavor symmetries and has no effect on the matrix structure of Σ, as we expect for a correctly implemented temperature dependence. Its only effect is to change the overall magni-

tude of the condensates. This result agrees with the static part of the chiral Lagrangian derived in [13], which is (in our notation):

$$\mathcal{L}_{\rm stat}(\Sigma) = -\frac{F^2 m_\pi^2}{2}\mathrm{Tr}(\Sigma M + \Sigma^\dagger M^\dagger) - \frac{F^2}{4}\mathrm{Tr}(\Sigma^\dagger(\mu_I I_3 + \mu_B B)\Sigma(\mu_I I_3 + \mu_B B)). \tag{4.16}$$

This Lagrangian has been analyzed in detail in [13]. In the remainder of this subsection we give a brief review of the main results of this paper. Let us first discuss the symmetries of the Lagrangian. In the vacuum, the $\mathrm{SU}(2N_f)$ symmetry is spontaneously broken according to $\mathrm{SU}(2N_f) \to \mathrm{Sp}(2N_f)$, in the same way as it is broken by the mass term. At nonzero baryon chemical potential, the symmetry is $\mathrm{SU}(N_f) \times \mathrm{SU}(N_f)$ and is broken by the diquark condensate to $\mathrm{Sp}(N_f) \times \mathrm{Sp}(N_f)$. If in addition the mass is nonzero, the symmetry at $\mu \neq 0$ is $\mathrm{U}(1) \times \mathrm{SU}(N_f)$ which is spontaneously broken by the diquark condensate to $\mathrm{Sp}(N_f)$ [10].

The mass term and the terms for baryon and isospin chemical potential are individually minimized by Σ-matrices corresponding to a chiral condensate, a diquark condensate and a pion condensate, respectively. To minimize the Lagrangian, we use an ansatz consisting of a linear combination of these individual minima,

$$\Sigma = \cos\alpha\Sigma_\sigma + \sin\alpha(\cos\eta\Sigma_\Delta + \sin\eta\Sigma_\rho), \tag{4.17}$$

which is again antisymmetric and unitary. These matrices, which correspond to the source terms introduced in (3.6), (3.7), and (4.4), are given by

$$\Sigma_\sigma = \begin{pmatrix} 0 & -1 & 0 & 0 \\ 1 & 0 & 0 & 0 \\ 0 & 0 & 0 & -1 \\ 0 & 0 & 1 & 0 \end{pmatrix}, \quad \Sigma_\Delta = \begin{pmatrix} 0 & 0 & -i & 0 \\ 0 & 0 & 0 & -i \\ i & 0 & 0 & 0 \\ 0 & i & 0 & 0 \end{pmatrix}, \quad \Sigma_\rho = \begin{pmatrix} 0 & 0 & 0 & -1 \\ 0 & 0 & -1 & 0 \\ 0 & 1 & 0 & 0 \\ 1 & 0 & 0 & 0 \end{pmatrix}. \tag{4.18}$$

Although the baryon chemical potential term is invariant under the $U_B(1)$ rotations generated by B, this symmetry is spontaneously broken by the diquark condensate, violating baryon number conservation and giving rise to a massless Goldstone boson [26]. In the same way, the pion condensate breaks the I_3 generated symmetry, which also leads to a violation of isospin number conservation and a Goldstone boson [4,53].

Using the ansatz for Σ, the effective Lagrangian (4.6) becomes

$$\mathcal{L} = nN_f[1 + \log G^2 - 2mG\cos\alpha + G^2(\cos^2\alpha(\mu_I^2 + \mu_B^2) - \sin^2\alpha\cos(2\eta) \times (\mu_B^2 - \mu_I^2)) + \mathcal{O}(\epsilon^2)]. \tag{4.19}$$

When this is minimized with respect to η, for $\alpha \neq 0$ and $\mu_B^2 \neq \mu_I^2$, we find

$$\eta = 0 \quad \text{for} \quad \mu_B^2 > \mu_I^2, \qquad \eta = \frac{\pi}{2} \quad \text{for} \quad \mu_B^2 < \mu_I^2, \tag{4.20}$$

where the first case corresponds to the presence of a diquark condensate, and the second to that of a pion condensate. Thus, there is a first order transition between these two phases on the lines $\mu_B^2 = \mu_I^2$. Minimizing now with respect to α, we find

$$\begin{aligned} &\cos\alpha = 1 \quad \text{for} \quad \mu_B^2 < \frac{m}{2G} \quad \text{and} \quad \mu_I^2 < \frac{m}{2G}, \\ &\cos\alpha = \frac{m}{2G}\frac{1}{\mu_B^2} \quad \text{for} \quad \mu_B^2 > \frac{m}{2G} \quad \text{and} \quad \mu_B^2 > \mu_I^2, \\ &\cos\alpha = \frac{m}{2G}\frac{1}{\mu_I^2} \quad \text{for} \quad \mu_I^2 > \frac{m}{2G} \quad \text{and} \quad \mu_B^2 < \mu_I^2. \end{aligned} \tag{4.21}$$

Since the critical chemical potential for the condensation of Goldstone bosons in our convention is half the pion mass, $\mu_c = m_\pi/2$, we can identify to this order in the expansion parameter

$$m_\pi = \sqrt{\frac{2m}{G}}. \tag{4.22}$$

From the analysis of the chiral Lagrangian we thus have obtained the following picture of the phase diagram at zero temperature: below a chemical potential of half the pion mass, the chiral condensate is constant. Above this critical chemical potential, depending on the relative magnitude of isospin and baryon chemical potential, pion or diquark condensation sets in and the chiral condensate drops quickly. The phases of pion and diquark condensation phases are separated by first order transition lines at $\mu_I^2 = \mu_B^2$.

C. Effective potential

We now wish to analyze the random matrix model to all orders in the mass and chemical potentials. To this end, we make an ansatz for the matrix A, and obtain an effective potential for the condensates in our model. As in the case for three colors, the ansatz for A is guided by two observations: From chiral perturbation theory, we know that above a critical chemical potential pion and diquark states will condense. We also expect that the presence of two

flavor dependent chemical potentials, which explicitly breaks the flavor symmetry, will lead to a different behavior of the chiral condensates for the two flavors. This leads to the following ansatz for A,

$$A = \begin{pmatrix} 0 & -\sigma_1 & -i\Delta & -\rho \\ \sigma_1 & 0 & -\rho & -i\Delta \\ i\Delta & \rho & 0 & -\sigma_2 \\ \rho & i\Delta & \sigma_2 & 0 \end{pmatrix}. \tag{4.23}$$

With this ansatz, evaluating the determinant we obtain the effective potential for the condensates:

$$\frac{1}{n}\mathcal{L} = G^2(\sigma_1^2 + \sigma_2^2 + 2\Delta^2 + 2\rho^2) - \frac{1}{2}\mathrm{Tr}\log Q_+ Q_-, \tag{4.24}$$

where

$$\begin{aligned}\det Q_\pm = \{&[(\sigma_1 + m + \mu_1 \pm iT)(\sigma_2 + m - \mu_2 \mp iT) + \rho^2 + \Delta^2] \times [(\sigma_1 + m - \mu_1 \pm iT)(\sigma_2 + m + \mu_2 \mp iT) \\ &+ \rho^2 + \Delta^2] + 4\Delta^2\mu_1\mu_2\}\{[(\sigma_1 + m - \mu_1 \mp iT)(\sigma_2 + m + \mu_2 \pm iT) + \rho^2 + \Delta^2] \\ &\times [(\sigma_1 + m + \mu_1 \mp iT)(\sigma_2 + m - \mu_2 \pm iT) + \rho^2 + \Delta^2] + 4\Delta^2\mu_1\mu_2\},\end{aligned} \tag{4.25}$$

Although $\det Q_+$ and $\det Q_-$ are complex conjugate to each other by construction, they turn out to be real themselves. With the ansatz (4.23) the symmetry (4.8) corresponds to the interchange (for $j = \lambda = 0$)

$$\Delta \to \rho, \qquad \rho \to -\Delta, \qquad \mu_2 \to -\mu_2. \tag{4.26}$$

The effective potential (4.24) is indeed invariant under this symmetry, as well as the interchange of the flavor indices, and $\mu_f \to -\mu_f$ for both $f = 1, 2$. These are the symmetries of the QCD partition function, as shown in Sec. II. They allow us to restrict our study to one half quadrant of the μ_B–μ_I-plane. The other sectors of the phase diagram are easily obtained by applying these symmetries. The transition between the phases with diquark and pion condensation must necessarily be of first order and take place on the lines $\mu_I^2 = \mu_B^2$.

V. PHASE DIAGRAM

In this section, we will determine the complete phase diagram of the random matrix model in the space of the chemical potentials, μ_B and μ_I, and the temperature T. To this end, we solve the saddle point equations

$$\frac{\partial\mathcal{L}}{\partial\sigma_1} = 0, \qquad \frac{\partial\mathcal{L}}{\partial\sigma_2} = 0, \qquad \frac{\partial\mathcal{L}}{\partial\rho} = 0, \qquad \frac{\partial\mathcal{L}}{\partial\Delta} = 0 \tag{5.1}$$

and determine the expectation values of all the condensates in the saddle point approximation. For vanishing temperature, we will obtain analytical solutions in the chiral limit as well as for finite quark mass. For nonzero temperature, we will present analytical results only in the chiral limit and study the potential numerically for finite quark mass.

A. Chiral limit at zero temperature

First, we investigate the phase diagram in the μ_1–μ_2 chemical potential plane at temperature $T = 0$. In the chiral limit, the Goldstone bosons arising from the spontaneous breaking of the chiral symmetry are exactly massless. Since all Goldstone bosons carry a charge that couples to one of the chemical potentials, this has a direct bearing on the phase diagram. At zero temperature, the chiral condensate will be rotated completely into a bosonic condensate as soon as one of the chemical potentials becomes nonzero.

a. Chiral condensates and chiral restoration transition—In the phase where the bosonic condensates vanish, $\Delta = \rho = 0$, the effective potential greatly simplifies and becomes a sum over the contributions of the chiral condensates for the two flavors,

$$\frac{1}{n}\mathcal{L} = \sum_{f=1,2} G^2\sigma_f^2 - \frac{1}{2}\log(\sigma_f^2 - \mu_f^2)^2. \tag{5.2}$$

Exactly as in the case of three-color QCD, the saddle point equations

$$\sigma_f[G^2(\sigma_f^2 - \mu_f^2) - 1] = 0, \qquad f = 1, 2, \tag{5.3}$$

have the solutions

$$\sigma_f = 0, \qquad f = 1, 2, \tag{5.4}$$

$$\sigma_f^2 = \frac{1}{G^2} + \mu_f^2, \qquad f = 1, 2, \tag{5.5}$$

which correspond to a phase with restored and broken chiral symmetry, in this order. The contributions to the free energy for one flavor are

$$\Omega_f(\mu_f) = -\log\mu_f^2 \tag{5.6}$$

$$\Omega_f(\mu_f) = 1 + \log G^2 + \mu_f^2 G^2, \tag{5.7}$$

for each of these phases, respectively. The chiral symmetry restoration phase transitions take place at the chemical potential for which the two free energies coincide. It is given by the solution of

$$1 + \mu_f^2 G^2 + \log\mu_f^2 G^2 = 0. \tag{5.8}$$

We note that this condition depends on only one of the two

chemical potentials and is strictly constant in the other. The behavior of the two flavors in these phases is completely independent. This changes only in the presence of either a pion or diquark condensate, which couples both flavors. As a result, the phases with one nonzero chiral condensate extend along the chemical potential axes. Only in the center of the phase diagram, where these strips overlap, could a phase exist for which both chiral condensates are nonzero.

b. Phases with bosonic condensates—At the point $\mu_1 = \mu_2 = 0$, the solution of the saddle point equation is degenerate. It satisfies $\sigma_1\sigma_2 + \Delta^2 + \rho^2 = 1/G^2$, without a preference for a specific direction in the space of the condensates. Because of the absence of flavor symmetry breaking terms we expect $\sigma_1 = \sigma_2$. This is the only point where all condensates can be simultaneously nonzero.

In the chiral limit, the chiral condensates vanish at nonzero chemical potential in the presence of a bosonic condensate. As we argued above, the phases with diquark and pion condensation must be separated by a first order transition. This is confirmed by the saddle point equation: the only solution for which $\Delta \neq 0$ *and* $\rho \neq 0$ requires that either $\mu_1 = 0$ or $\mu_2 = 0$, which is equivalent to $\mu_I^2 = \mu_B^2$ and thus coincides with the expected first order transition line. Therefore, we always have either a pion or a diquark condensate, and the effective potential in these two cases is reduced to

$$\frac{1}{n}\mathcal{L} = 2G^2\rho^2 - \log(\rho^2 - \mu_1\mu_2)^2, \tag{5.9}$$

$$\frac{1}{n}\mathcal{L} = 2G^2\Delta^2 - \log(\Delta^2 + \mu_1\mu_2)^2. \tag{5.10}$$

The corresponding saddle point equations become

$$G^2\rho(\rho^2 - \mu_1\mu_2) - \rho = 0, \tag{5.11}$$

$$G^2\Delta(\Delta^2 + \mu_1\mu_2) - \Delta = 0, \tag{5.12}$$

and have the respective solutions

$$\rho = 0, \qquad \rho^2 = \frac{1}{G^2} + \mu_1\mu_2 \tag{5.13}$$

$$\Delta = 0, \qquad \Delta^2 = \frac{1}{G^2} - \mu_1\mu_2. \tag{5.14}$$

Second order phase transition lines are given by the conditions $\mu_1\mu_2 = -1/G^2$ and $\mu_1\mu_2 = 1/G^2$. The free energies for the two solutions are

$$\Omega_\rho = 2(1 + \log G^2 + \mu_1\mu_2 G^2), \tag{5.15}$$

$$\Omega_\Delta = 2(1 + \log G^2 - \mu_1\mu_2 G^2). \tag{5.16}$$

By comparing the free energies, we observe that in the quadrants with $\mu_1\mu_2 > 0$, the diquark condensate is nonzero, and that for $\mu_1\mu_2 < 0$ the solution with a pion condensate has the lower free energy. Equating the free energies, we confirm again that first order transition lines are given by $\mu_1\mu_2 = 0$.

c. Phase diagram—To find the complete phase diagram, we use the results we obtained directly for the second order phase transitions, and we compare the free energies of all phases to determine the first order transitions. We conclude that, for massless quarks, phases with condensed bosons are always favored above a phase where both chiral condensates are nonvanishing. In addition to the first order transitions between the pion and diquark condensate phases, we find first order transitions from these to the phases where only one of the chiral condensates is different from zero.

The phase diagram is shown in Fig. 1. At the origin, the solution to the saddle point equation is degenerate, and only the magnitude of the condensates is fixed. From the origin, a pion condensation phase extends into the quadrants where $\mu_1\mu_2 < 0$ ($\mu_I^2 > \mu_B^2$), and a diquark condensation phase extends into the quadrants where $\mu_1\mu_2 > 0$ ($\mu_I^2 < \mu_B^2$). The domain of these phases is limited by a line of second order transitions (see dashed curve in Fig. 1), which in each quadrant is given by the solutions of

$$1 \pm G^2\mu_1\mu_2 = 0. \tag{5.17}$$

These transitions can be interpreted as saturation transitions which also occur in lattice QCD because of the finite number of available fermionic states [27]. Our saturation transition is somewhat different. Because we are working

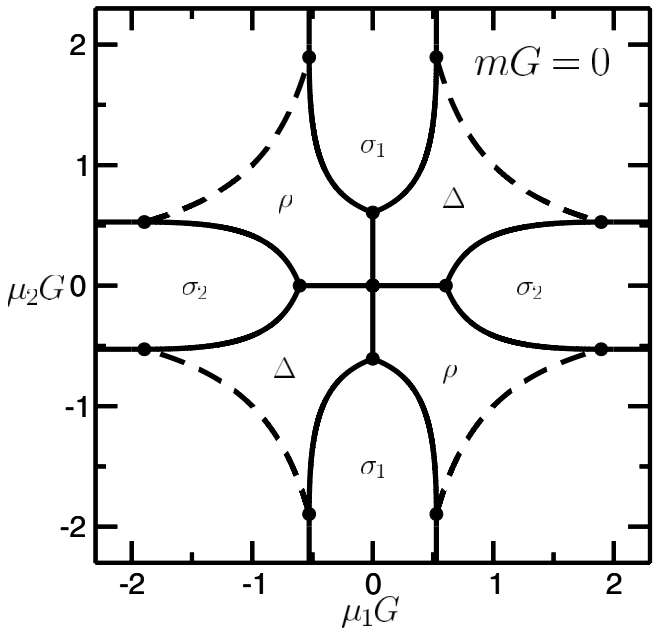

FIG. 1. Phase diagram in the μ_1–μ_2-plane at $T = 0$ and vanishing quark mass $mG = 0$. First (second) order transitions are indicated by solid (dashed) lines. Phases are labeled by the nonvanishing condensates. All condensates vanish in the corner regions, where chiral symmetry is restored.

in the thermodynamic limit, the number of available states is infinite as well. However, since the level spacing of the relevant matrices $\sim 1/n$, the support of the spectrum remains compact. It is the nonanalyticity that occurs because of the extreme edges of the spectrum that gives rise to the saturation transition. The phases with broken chiral symmetry and only *one* of the chiral condensates nonzero appear along both chemical potential axes. They are separated from the Goldstone condensation phases by first order transition lines.

The phase diagram exhibits a four-fold symmetry, along both the μ_B- and the μ_I- axis. This is in contrast to the twofold symmetry with respect to the μ_B-axis that we found in the phase diagram of three-color QCD, where only a pion condensate appears [34]. Fundamentally, this is due to the flavor symmetry in the two-color case which is enlarged beyond the symmetry in the three-color case. However, the upper-left quadrant in the μ_B–μ_I-plane is strictly identical in our random matrix model for both two and three colors [34]. The important point is that both chemical potentials couple to Goldstone bosons of the theory. Therefore, the two chemical potential terms in the present case are on equal footing. They lead to two different possible symmetry breaking patterns. For three colors, there is only one chemical potential term, since only the isospin chemical potential couples to the Goldstone modes, and thus there is only one way to break the flavor symmetry.

B. Nonzero quark mass at $T = 0$

The phase diagram in the presence of a finite quark mass differs from the one obtained in the chiral limit. As in the case of three colors, this is due to two effects: First, the chiral condensate becomes nonzero because of the explicit breaking of chiral symmetry. Because of this, phase transitions may turn into crossover transitions. Second, previously exactly massless Goldstone bosons become massive. This primarily affects the low-energy regions of the phase diagram. In addition, the Goldstone condensation phases become qualitatively different and are now mixed phases with nonzero chiral condensates. In spite of this, at zero temperature we can still solve the saddle point equations exactly, and we will give the results below.

a. Chiral condensation phases—For a small quark mass, the behavior of the chiral condensate is still dominated by the spontaneous breaking of the chiral symmetry. Thus, a natural way to treat the chiral condensates in this case is to expand in the quark mass about the solutions for $m = 0$.

The effective potential that describes the phases without bosonic condensates is given by

$$\frac{1}{n}\mathcal{L} = \sum_{f=1,2} G^2\sigma_f^2 - \frac{1}{2}\log[(\sigma_f + m)^2 - \mu_f^2]^2. \quad (5.18)$$

For each flavor we have to solve the saddle point equation

$$G^2\sigma_f[(\sigma_f + m)^2 - \mu_f^2] - (\sigma_f + m) = 0. \quad (5.19)$$

As expected, the solution $\sigma_f = 0$ no longer exists, and we find by expanding in m (without assumptions about the magnitude of μ_f) the new solution

$$\sigma_f = -\frac{1}{1 + \mu_f^2 G^2} m + \mathcal{O}(m^3). \quad (5.20)$$

Expanding in mG in the phase with spontaneously broken chiral symmetry around the second solution with $G^2\sigma_f = \mathcal{O}(G)$, we find the solutions

$$G\sigma_f = \pm\sqrt{1 + \mu_f^2 G^2} + \left(\frac{1}{2(1 + \mu_f^2 G^2)} - 1\right)mG + \mathcal{O}(m^2G^2). \quad (5.21)$$

The respective free energies for one flavor of these two phases with spontaneously broken and restored chiral symmetry are to lowest order in m given by

$$\Omega_f = 1 + \mu_f^2 G^2 + \log G^2 \mp 2mG\sqrt{1 + \mu_f^2 G^2}, \quad (5.22)$$

$$\Omega_f = -\log\mu_f^2. \quad (5.23)$$

If these two phases are not separated by a Bose-condensation phase and meet directly, the chiral restoration transition is of first order. The chemical potential at the transition is obtained by matching the free energies of the two phases. We find

$$\mu'_{f,c}G = \mu_c G\left(1 + \frac{mG}{1 + \mu_c^2 G^2} + \mathcal{O}(m^2G^2)\right), \quad (5.24)$$

where $\mu_c G$ is the critical chemical potential in the chiral limit determined from (5.8). The shift in the chiral restoration transition is proportional to the quark mass m.

b. Goldstone boson condensation phases—For finite quark mass, the critical chemical potential for condensation of Goldstone bosons becomes nonzero due to their finite mass. The symmetry with regards to the chemical potentials μ_I and μ_B remains unaffected. In particular, above the critical chemical potential, we still expect to see either a phase with diquark condensation or one with pion condensation depending on the relative magnitude of these two potentials, and a first order transition separating them. Since the results for both Goldstone condensation phases are related by this symmetry and are thus very similar, we will give explicit results for one half quadrant only.

In both phases, due to the finite quark mass, the chiral condensates do not vanish. Therefore, we have to solve three saddle point equations simultaneously, for the chiral condensates of both flavors and for either ρ or Δ. In the region in which $|\mu_I| > |\mu_B|$, we thus have $\Delta = 0$. The solutions of the saddle point equations are given by:

$$\sigma_1 = -m + \frac{m}{2}\frac{1}{G^2}\frac{1}{\mu_I^2 - m^2} + \frac{1}{2}m(\mu_B + \mu_I)\frac{\mu_B}{\mu_I^2},$$

$$\sigma_2 = -m + \frac{m}{2}\frac{1}{G^2}\frac{1}{\mu_I^2 - m^2} + \frac{1}{2}m(\mu_B - \mu_I)\frac{\mu_B}{\mu_I^2},$$

$$\rho^2 + \sigma_1\sigma_2 = \frac{1}{G^2} + \mu_B^2 - \mu_I^2 + m^2 - m^2\frac{\mu_B^2}{\mu_I^2}. \tag{5.25}$$

From the relation between the chiral and the pion condensate, we find the explicit result for ρ,

$$\rho^2 = \mu_B^2 - \mu_I^2 + \mu_I^2\frac{1}{G^2}\frac{1}{\mu_I^2 - m^2} - \frac{m^2}{4}\frac{1}{G^4}\frac{1}{(\mu_I^2 - m^2)^2} - m^2\frac{\mu_B^2}{\mu_I^2}\left(\frac{1}{4\mu_I^2}(\mu_B^2 - \mu_I^2) + \frac{1}{2}\frac{1}{G^2}\frac{1}{\mu_I^2 - m^2}\right). \tag{5.26}$$

The difference between the two chiral condensates depends on the ratio of μ_B and μ_I:

$$\sigma_1 - \sigma_2 = m\frac{\mu_B}{\mu_I}. \tag{5.27}$$

The free energy of this phase is given by

$$\Omega_\rho(m, \mu_B, \mu_I) = 2(1 + \log G^2 + (\mu_B^2 - \mu_I^2)G^2 + m^2G^2) - m^2G^2\frac{\mu_B^2}{\mu_I^2} - \log\left(\frac{\mu_I^2}{\mu_I^2 - m^2}\right). \tag{5.28}$$

The condition $\rho^2 = 0$ describes a line of second order phase transitions at which the bosonic condensate vanishes. For finite quark mass, this condition has more than one solution. For $\mu_B = 0$, the two solutions for μ_I^2 are

$$\mu_{Ic}^2 G^2 = \frac{mG}{2} + \frac{5}{8}m^2G^2 + \mathcal{O}(m^3G^3), \tag{5.29}$$

$$\mu_{Ic}^2 G^2 = 1 + \frac{3}{4}m^2G^2 + \mathcal{O}(m^4G^4). \tag{5.30}$$

We note that the solution for which $\mu_{Ic}^2G^2 = mG/2 + \mathcal{O}(m^2G^2)$ agrees to leading order with the result which was obtained from chiral perturbation theory [9,10]. For chemical potentials below the critical value of μ_B, at which diquark condensation occurs, the pion mass is expected to be independent from μ_B [13]. Thus, the critical value for μ_I should be exactly constant as a function of μ_B. In our random matrix model we find that μ_{Ic} is only approximately constant as a function of μ_B. This is due to the fact that, in random matrix models, the chemical potential affects the condensates already below the threshold, even at zero temperature [6,47,51]. In [6,51] it was thus argued that the random matrix result should be interpreted as the critical contribution to the free energy, on top of a noncritical part not contained in the model.

For small baryon chemical potential, small isospin chemical potential and quark mass, the chiral condensates in the pion condensation phase become

$$\sigma_1 = \sigma_2 = \sigma = \frac{m}{2G^2\mu_I^2} + \mathcal{O}(m), \tag{5.31}$$

$$\sigma^2 + \rho^2 = \frac{1}{G^2} + \mathcal{O}(m), \tag{5.32}$$

which agrees with the results (4.21) obtained in chiral perturbation theory. In this region of the phase diagram the effects of a finite quark mass are most significant. For large values of the chemical potentials both the pion and diquark condensates vanish for any value of the quark mass. The second order transition to this phase is to leading order independent of the quark mass.

c. Phase diagram—As in the chiral limit, in order to obtain the complete phase diagram we combine the results for the second order transitions with an analysis of the free energies of the different phases. The resulting phase diagram in the μ_1–μ_2-plane is shown in Fig. 2 for a quark mass of $mG = 0.1$. The four-fold symmetry remains the same as in the case of $mG = 0$. In particular, the transitions between the phases with the different Goldstone boson condensates are still of first order. The main difference from the chiral limit is the appearance of a phase in the center of the phase diagram in which the chiral condensates for both flavors are nonzero. This is a consequence of the finite critical chemical potential for the condensation of bosons with a finite mass.

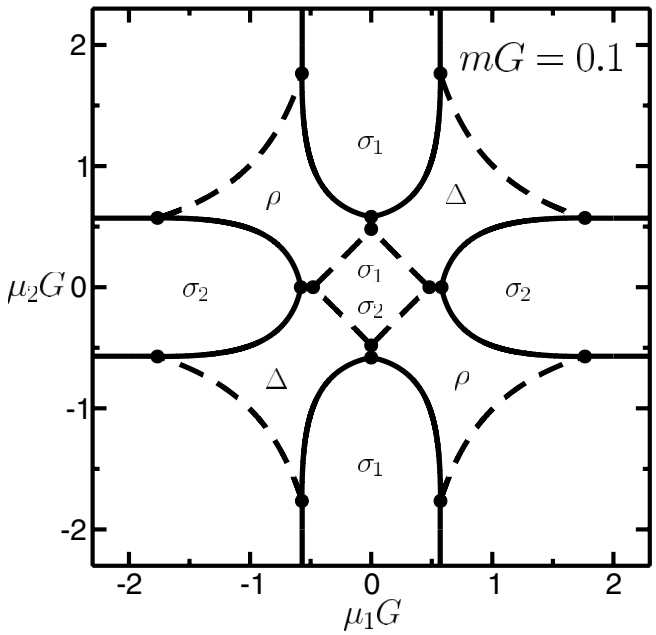

FIG. 2. Phase diagram in the μ_1–μ_2-plane at $T = 0$ for a finite quark mass $mG = 0.1$. First (second) order transitions are indicated by solid (dashed) lines. The different phases are labeled by the nonvanishing condensates or the condensates which have large expectation values. The finite quark mass leads to a phase with chiral condensation only in the center of the phase diagram. In the corner regions, both the diquark condensate and the pion condensate vanish, and the chiral condensates are of $\mathcal{O}(m)$.

A second effect of the finite quark masses is that the chiral restoration transitions outside the regions of Bose condensation are shifted slightly from their positions in the chiral limit. As can be seen from (5.24), the correction is of order mG. Thus, while changing the nature of the phase transition considerably in the regions of low chemical potential in the center of the phase diagram, a finite quark mass has only a small effect on the phase diagram at large chemical potential.

For leading order in the mass expansion, we find that the first order transition between the phases with $\rho \neq 0$ and $\Delta \neq 0$ disappears at the point $1 + \log 2mG = 0$. Therefore, for masses larger than $mG \sim 0.184$, the pion and diquark condensation phases are not contiguous anymore. In this case, if either μ_1 or μ_2 is kept small and the chemical potential for the other quark flavor is increased, one encounters the chiral restoration transition without passing through either the pion or the diquark condensation phase.

Nonzero T at $m = 0$

1. The $\mu_I = 0$- and $\mu_B = 0$-planes

Since the presence of a temperature term does not change the symmetries, even at finite temperature the two phases with the different Goldstone condensates are still related by an interchange of the two chemical potentials. We can again treat both the pion and diquark condensation phases in parallel. In either the $\mu_I = 0$ or the $\mu_B = 0$ plane, the presence of only one of these chemical potentials restores the symmetry between the two quark flavors. Consequently, there is only one chiral condensate $\sigma = \sigma_1 = \sigma_2$. The results for the chiral phase transition were first obtained for $\mu_I = 0$ in [6]. The results in the plane $\mu_B = 0$ coincide with those for $N_c = 3$ at nonzero isospin chemical potential [34] where the same effective potential was found. Therefore, and mainly for completeness, we briefly review the main results. The result for the diquark condensate can be obtained by the simple substitution $\mu_I \rightarrow \mu_B$ and $\rho \rightarrow -\Delta$.

In the chiral limit the critical chemical potential for pion condensation of this model is independent of the temperature. For any nonzero value $|\mu_I| > 0$, the system will be immediately in the pion condensation phase (via a first order transition from the degenerate point $\mu_I = 0$). The effective potential for this phase is

$$\frac{1}{n}\mathcal{L} = 2G^2\rho^2 - \log[(\rho^2 + \mu_I^2 + T^2)^2], \tag{5.33}$$

and the saddle point equations are solved by

$$\rho^2 = \frac{1}{G^2} - \mu_I^2 - T^2, \tag{5.34}$$

$$\rho = 0. \tag{5.35}$$

The phase diagram is now simple: A second order transition line is given by the circle $G^2(\mu_I^2 + T^2) = 1$. The free energy of this phase with $\sigma_1 = \sigma_2 = 0$, given by

$$\Omega_\rho = 2[1 + \log G^2 - G^2(\mu_I^2 + T^2)], \tag{5.36}$$

is always lower than that of the chiral broken phase, and thus in the chiral limit, the chiral condensates do not appear in this plane (see the upper panel of Fig. 4). Therefore, the tricritical point of the chiral restoration transition found in the μ_B–T-plane at $\mu_I = 0$ for $N_c = 3$ [6] does not appear at all in the μ_I–T-plane given by $\mu_B = 0$. Using the symmetry of the phase diagram, we see that, in contrast to the case $N_c = 3$, for $N_c = 2$ this tricritical point is not present in the μ_B–T-plane with $\mu_I = 0$, either.

2. The complete μ_I–μ_B-plane at $T \neq 0$

In the chiral limit, we can still solve the saddle point equations analytically. Since the first order phase transition between the pion and diquark condensation phases is not affected by the temperature, we continue to have phases of pure diquark and pure pion condensation which meet at the first order transition lines $\mu_1 = 0$ or $\mu_2 = 0$ (i.e. $\mu_I = \pm\mu_B$). There are no phases in which a pion condensate or a diquark condensate coexists with a chiral condensate of any flavor.

a. Chiral condensation phases—The phase with only chiral condensation occurs along strips parallel to the $\mu_1 = 0$ or $\mu_2 = 0$ axis (see Fig. 1). In these phases only one of the chiral condensates is nonvanishing. The effective potential simplifies to a sum over two independent contributions of both flavors,

$$\frac{1}{n}\mathcal{L} = \sum_{f=1,2}\left\{G^2\sigma_f^2 - \frac{1}{2}\log[(\sigma_f^2 - \mu_f^2 + T^2)^2 + 4\mu_f^2T^2]\right\}, \tag{5.37}$$

and coincides with the effective potential found for QCD with three colors. For each of the two flavors, the chiral condensate depends only on the temperature and the chemical potential for that flavor. In the chiral limit, the magnitude of the chiral condensate is given by the solution of the saddle point equation

$$G^2\sigma_f\left[\sigma_f^4 - 2\left(\frac{1}{2G^2} + \mu_f^2 - T^2\right)\sigma_f^2 + \frac{1}{G^2}(\mu_f^2 - T^2) + (\mu_f^2 + T^2)^2\right] = 0. \tag{5.38}$$

Its solutions are given by [6]

$$\sigma_f = 0, \tag{5.39}$$

$$\sigma_f^2 = \frac{1}{2G^2} + \mu_f^2 - T^2 \pm \frac{1}{2G^2}\sqrt{1 - (4G^2\mu_f T)^2}, \tag{5.40}$$

and due to the solution $\sigma_f = 0$ a first order transition to the phase with restored chiral symmetry is possible. For any one flavor $f = 1, 2$, this first order transition takes place

where the free energies of the two solutions, given by

$$\Omega_f = -\log(\mu_f^2 + T^2), \tag{5.41}$$

$$\Omega_f = \frac{1}{2} + \log G^2 + G^2(\mu_f^2 - T^2) \pm \frac{1}{2}\sqrt{1 - (4G^2\mu_f T)^2} - \frac{1}{2}\log\left(\frac{1}{2} \pm \frac{1}{2}\sqrt{1 - (4G^2\mu_f T)^2}\right), \tag{5.42}$$

respectively, become equal. The solution $\sigma_f \neq 0$ with the negative square root is not a global minimum of the free energy, and is in fact never realized. We find that the solution $\sigma_f \neq 0$ approaches the solution $\sigma_f = 0$ at the second order phase transition line in the μ_f–T-plane given by

$$(\mu_f^2 - T^2) + G^2(\mu_f^2 + T^2)^2 = 0. \tag{5.43}$$

The tricritical point, where the phase transition line changes from first to second order, appears where the coefficients of σ_f and σ_f^3 in (5.38) vanish. We find [6]

$$\mu_{f,3}^2 G^2 = \frac{\sqrt{2} - 1}{4}, \qquad f = 1, 2, \qquad T_3^2 G^2 = \frac{\sqrt{2} + 1}{4}. \tag{5.44}$$

Since these results are independent of the chemical potential for the other flavor, all transition lines are straight lines in the μ_1–μ_2-plane at fixed temperature. In fact, the transition lines for one flavor in this plane have to be perpendicular to the corresponding lines of the other flavor.

b. Goldstone boson condensation phases—Once again relying on the symmetry of the effective potential (4.24), it is sufficient to analyze the pion condensate. Results for the diquark condensate simply follow from interchanging μ_I and μ_B. The effective potential in the pion condensation phase at finite temperature is given by

$$\frac{1}{n}\mathcal{L} = 2G^2\rho^2 - \log[(\rho^2 - \mu_B^2 + \mu_I^2 + T^2)^2 + 4\mu_B^2 T^2]. \tag{5.45}$$

To explore the structure of the boundaries of the domain of this phase, we analyze the saddle point equation

$$G^2\rho\Big[\rho^4 - 2\Big(\frac{1}{2G^2} + \mu_B^2 - \mu_I^2 - T^2\Big)\rho^2 + (\mu_B^2 - \mu_I^2 - T^2)^2 + 4\mu_B^2 T^2 + \frac{1}{G^2}(\mu_B^2 - \mu_I^2 - T^2)\Big] = 0. \tag{5.46}$$

Besides the trivial solution $\rho = 0$, the saddle point equation has the solutions

$$\rho^2 = \frac{1}{2G^2} + \mu_B^2 - \mu_I^2 - T^2 \pm \frac{1}{2G^2}\sqrt{1 - (4G^2\mu_B T)^2}, \tag{5.47}$$

of which only the one with the positive sign in front of the square root is a minimum of the free energy. A second order transition line is given by the condition that this solution coincides with the trivial solution,

$$(\mu_B^2 - \mu_I^2 - T^2)^2 + 4\mu_B^2 T^2 + \frac{1}{G^2}(\mu_B^2 - \mu_I^2 - T^2) = 0. \tag{5.48}$$

There is always the possibility of a first order transition to a phase with $\rho = 0$. Indeed, for a certain range of parameters, where the coefficients of both ρ^3 and ρ in Eq. (5.46) vanish, there exists a tricritical point at which the transition changes order. But when the complete phase diagram is considered, including all other condensates, the solutions that lead to this tricritical point do not appear: at this point the free energy of one of the chiral condensation phases is lower than that of the pion condensation phase, and a first order transition takes place before the point is reached. The free energy in the pion condensation phase is given by

$$\Omega_\rho = 2\Big\{\frac{1}{2} + \log G^2 + G^2(\mu_B^2 - \mu_I^2 - T^2) + \frac{1}{2}\sqrt{1 - (4G^2\mu_B T)^2} - \frac{1}{2}\log\Big[\frac{1}{2} + \frac{1}{2}\sqrt{1 - (4G^2\mu_B T)^2}\Big]\Big\}, \tag{5.49}$$

and we determine the complete phase diagram by comparing the free energies of the different phases. Using the symmetry (4.8), all the above results also apply to the diquark condensate.

c. Phase diagram—At finite temperature, the phase diagram in the μ_1-μ_2 plane still has the four-fold symmetry as seen at $T = 0$ in Fig. 1. As can be seen from the second order transition condition (5.48), the boundaries of the regions with diquark condensation or pion condensation move gradually towards the origin $\mu_B = \mu_I = 0$ with increasing temperature, and shrink rapidly to a point when TG approaches $TG = 1$. The regions with a nonzero chiral condensate also shrink gradually with increasing temperature. When the temperature reaches the tricritical point given by Eq. (5.44), the transition to the chirally restored region becomes second order. As the temperature approaches $TG = 1$ this region rapidly collapses onto the axes $\mu_1 = 0$ and $\mu_2 = 0$. All condensates vanish and the symmetries are completely restored for $TG \geq 1$.

D. Finite quark mass at nonzero T

In general, for $m \neq 0$ the saddle point equations cannot be solved analytically when μ_I, μ_B and T are all different from zero. However, as outlined in the previous section, the symmetries of the partition function under an interchange of the chemical potentials for the two flavors, or a change in their sign, are unaffected by the presence of the temperature term. Thus, the four symmetry axes $\mu_I = 0$, $\mu_B = 0$ and $\mu_I = \pm\mu_B$ remain at finite temperature, and

the first order transitions between the condensates Δ and ρ at $\mu_I = \pm\mu_B$ remain. The structure of the phase diagram in this case can be deduced from the analytical results at $T = 0$ and from the planes where one of the chemical potentials vanishes.

1. The $\mu_B = 0$- plane

Although an analytical solution of the saddle point equations is not possible for both chemical potentials and the temperature nonzero, in order to have a complete picture of the phase diagram it is instructive to consider the plane $\mu_B = 0$. Here, of course, the chiral condensates for both flavors coincide again. This region of the phase diagram has been studied at zero temperature in [4,13] by means of a chiral Lagrangian for small values of μ_I. Finite temperature effects have been included in a one-loop calculation in chiral perturbation theory in [12] and in the random gauge model of [51].

a. Chiral condensate—Below the critical value of μ_I, chiral symmetry is broken by the chiral condensate, and at high temperature it is restored after a crossover transition. For $m \neq 0$, it is most transparent to solve the saddle point equations for the chiral condensate by expanding in the quark mass m. In the broken phase, the chiral condensate $\sigma = \sigma_1 = \sigma_2$ is given by

$$\sigma = \sigma_0 + m\frac{1}{2\sigma_0^2}\frac{\sigma_0^2 - \mu_I^2 + T^2 - 8G^2T^2\mu_I^2}{1 - (4G^2\mu_I T)^2} - m + \mathcal{O}(m^2) \tag{5.50}$$

where σ_0 is the solution of the saddle point equation for $m = 0$,

$$\sigma_0^2 = \frac{1}{2G^2} + \mu_I^2 - T^2 + \frac{1}{2G^2}\sqrt{1 - (4G^2\mu_I T)^2}. \tag{5.51}$$

With increasing temperature, the chiral condensate decreases. In the high temperature phase, the chiral condensate can be expanded about the trivial solution (5.39) as

$$\sigma = -m\frac{\mu_I^2 - T^2}{G^2(\mu_I^2 + T^2)^2 + \mu_I^2 - T^2} + \mathcal{O}(m^3). \tag{5.52}$$

b. Pion condensate—As in the case $T = 0$, for finite quark mass the chiral condensate does not vanish in the pion condensation phase. In this mixed phase, we can solve the saddle point equations analytically. The solution given by

$$\sigma = -m + \frac{m}{2G^2}\frac{1}{\mu_I^2 - m^2}, \tag{5.53}$$

$$\sigma^2 + \rho^2 = \frac{1}{G^2} + m^2 - \mu_I^2 - T^2 \tag{5.54}$$

was first obtained for diquark condensation [51]. We notice that the chiral condensate is completely independent of the temperature, and only the total magnitude $\sigma^2 + \rho^2$ of the condensates decreases with increasing temperature. At zero temperature these equations describe the rotation of a chiral condensate into a pion condensate for increasing μ_I. The explicit solution for the pion condensate obtained from (5.54) is given by

$$\rho^2 = \frac{1}{G^2}\frac{\mu_I^2}{\mu_I^2 - m^2} - \frac{1}{4G^4}\frac{m^2}{(\mu_I^2 - m^2)^2} - \mu_I^2 - T^2. \tag{5.55}$$

The phase with $\rho \neq 0$ is bounded by a second order line at which ρ vanishes:

$$\mu_I^2(\mu_I^2 - m^2) - \frac{1}{4}m^2 - (\mu_I^2 + T^2)(\mu_I^2 - m^2)^2G^4 = 0. \tag{5.56}$$

An important observation is that in this case, as for $N_c = 3$, the boundary of the pion condensation phase is always a second order transition, and there is no tricritical point. The complete phase diagram for $\mu_B = 0$ is pictured in Fig. 4. In the μ_I–T-plane the critical endpoint of the first order chiral restoration transition does not appear, because its position is in the region where the pion condensation phase has a smaller free energy than the chiral condensation phase. We have shown [34] that in this plane even for large quark masses, the critical endpoint remains masked by the pion condensation phase.

2. The complete μ_I–μ_B-plane at $T \neq 0$

To obtain the full picture of the phase diagram at nonzero values for the two chemical potentials, the temperature and the quark mass, we solve the saddle point equations numerically. The results for the phase diagram are presented in Fig. 5. It is in complete agreement with the expectations from our discussion of the phase diagram at either $m = 0$ or $T = 0$: The finite quark mass mainly affects the phase diagram at low values of the chemical potentials, and the regions with either a diquark or a pion condensate shrink with increasing temperature and finally vanish for a temperature of order one, $TG = \mathcal{O}(1)$.

We wish to draw the attention to one particular detail of the phase diagram in our model. From Fig. 3, the diquark and pion condensation phases are no longer contiguous at the lines $\mu_1 = 0$ and $\mu_2 = 0$, and there is no first order transition between them. Instead, this region of the phase diagram is occupied once again by the chirally broken phases, and the chiral phase transition line reemerges. While the first order chiral transition line does not appear for $\mu_B = 0$ (and by symmetry not for $\mu_I = 0$, either), we thus find that for both μ_B and μ_I different from zero and an appropriate value of the quark mass this first order line and its critical endpoint can be observed. The phase diagram in the μ_B–T plane at an isospin chemical potential that is chosen to avoid the superfluid phases at low μ_B shares striking similarities with the phase diagram of QCD with

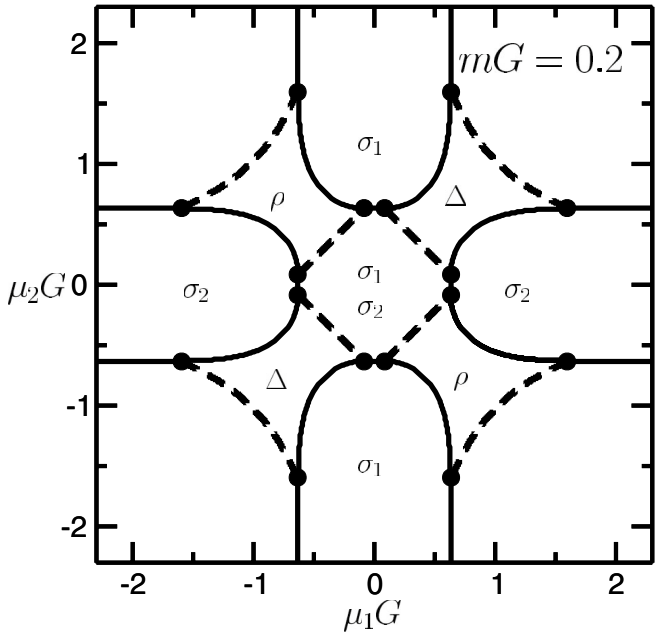

FIG. 3. Phase diagram in the μ_1–μ_2-plane at $T = 0$ for a finite quark mass $mG = 0.2$. First (second) order transitions are indicated by solid (dashed) lines. The different phases are labeled by the condensates which are nonvanishing or have a large expectation value. As described in the text, for a quark mass larger than $mG \sim 0.184$ the pion and diquark condensation phases no longer have a boundary in common. In contrast to the situation shown in Fig. 2, the chiral first order transition lines therefore appear also if one of the chemical potentials μ_f is small.

three colors at nonzero baryon and isospin chemical potentials.

3. The μ_B–T-plane at constant μ_I

To study the chiral phase transitions for both μ_B and μ_I nonzero in some more detail, we turn to the phase diagram in planes described by constant isospin chemical potential. Figure 6 shows the phase diagram in these μ_B–T-planes for fixed values of μ_I. The corresponding cuts through the phase diagram in the three parameters μ_I, μ_B, and T are perpendicular to the cuts at constant TG in Fig. 5. Since $\mu_1 = \mu_B + \mu_I$ and $\mu_2 = \mu_B - \mu_I$, planes at constant μ_I intersect the planes with constant T along lines parallel to the diagonal from the lower left-hand to the upper right-hand corners of the panels in Fig. 5.

In our analysis of the plane $\mu_B = 0$ and in Fig. 4 above, we have seen that the first order chiral phase transition and its critical endpoint are not present for any value of the quark mass, and by virtue of the symmetries this also holds for the plane given by $\mu_I = 0$, shown in the first panel of Fig. 6. But with increasing value of the isospin chemical potential the phase diagram in the μ_B–T-plane changes considerably: first, the first order chiral transition for $\sigma_1 \sim \langle \bar{u}u \rangle$ at large temperature and its critical endpoint reappear.

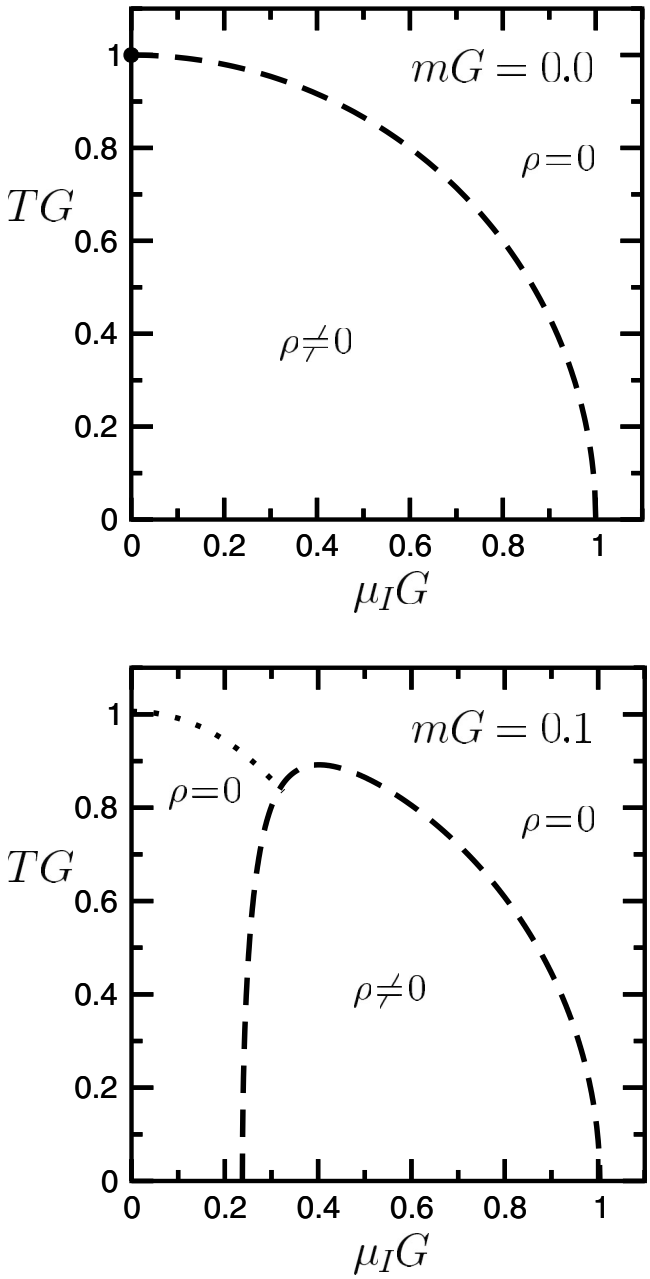

FIG. 4. Phase diagram in μ_I and T in the $\mu_B = 0$-plane, both for the chiral limit (top) and a finite quark mass $mG = 0.1$ (bottom). First (second) order transitions are indicated by solid (dashed) lines, the dotted lines in the case of finite quark mass mark the crossover.

With a further increase of μ_I, the chiral transition for σ_2 at large values of μ_B appears as well (see the second and following panels of Fig. 6). We have to caution, though, that for the second chiral condensate σ_2 this is possible only because of the saturation transition of the diquark condensate, which exists on the lattice as well as in our random matrix model. If μ_I is made larger still, the critical endpoint of the transition for σ_1 is once again swallowed

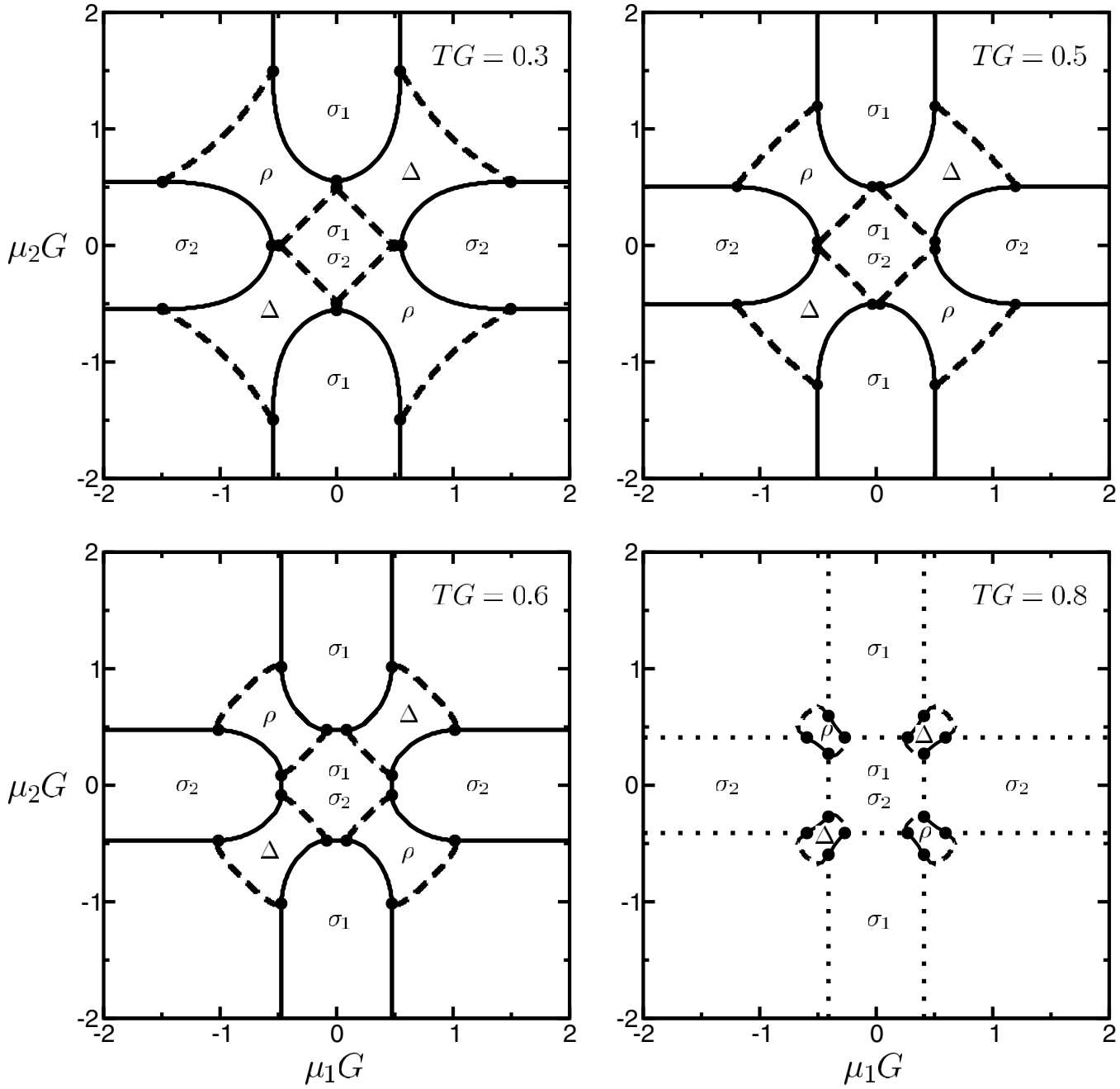

FIG. 5. Phase diagram in the μ_1–μ_2-plane at fixed values of TG and for a finite quark mass of $mG = 0.1$. Values for the temperature TG are given in the panels. First (second) order transitions are indicated by solid (dashed) lines, the dotted lines indicate a crossover. Phases are labeled by the nonvanishing condensates, resp. the condensates with large expectation values. In the corner regions, the pion and diquark condensates vanish, and both chiral condensates become small.

by the pion condensation phase (see last panel of Fig. 6, where this is about to take place).

For a quark mass $mG > 0.184$ and at any temperature, the diquark and pion superfluid phases are not contiguous. Therefore for a sufficiently large quark mass ($mG > 0.184$) and an isospin chemical potential that is small enough so that the pion superfluid phase is never reached and large enough so that the diquark superfluid phase is reached only at large μ_B, the structure of the phase diagram is as in Fig. 7. The resulting phase diagram is strikingly similar to the phase diagram of the random matrix model for QCD with three color at nonzero baryon and isospin chemical potentials [34].

VI. CONCLUSION

In this article, we have introduced a random matrix model with the symmetries of QCD with two colors and

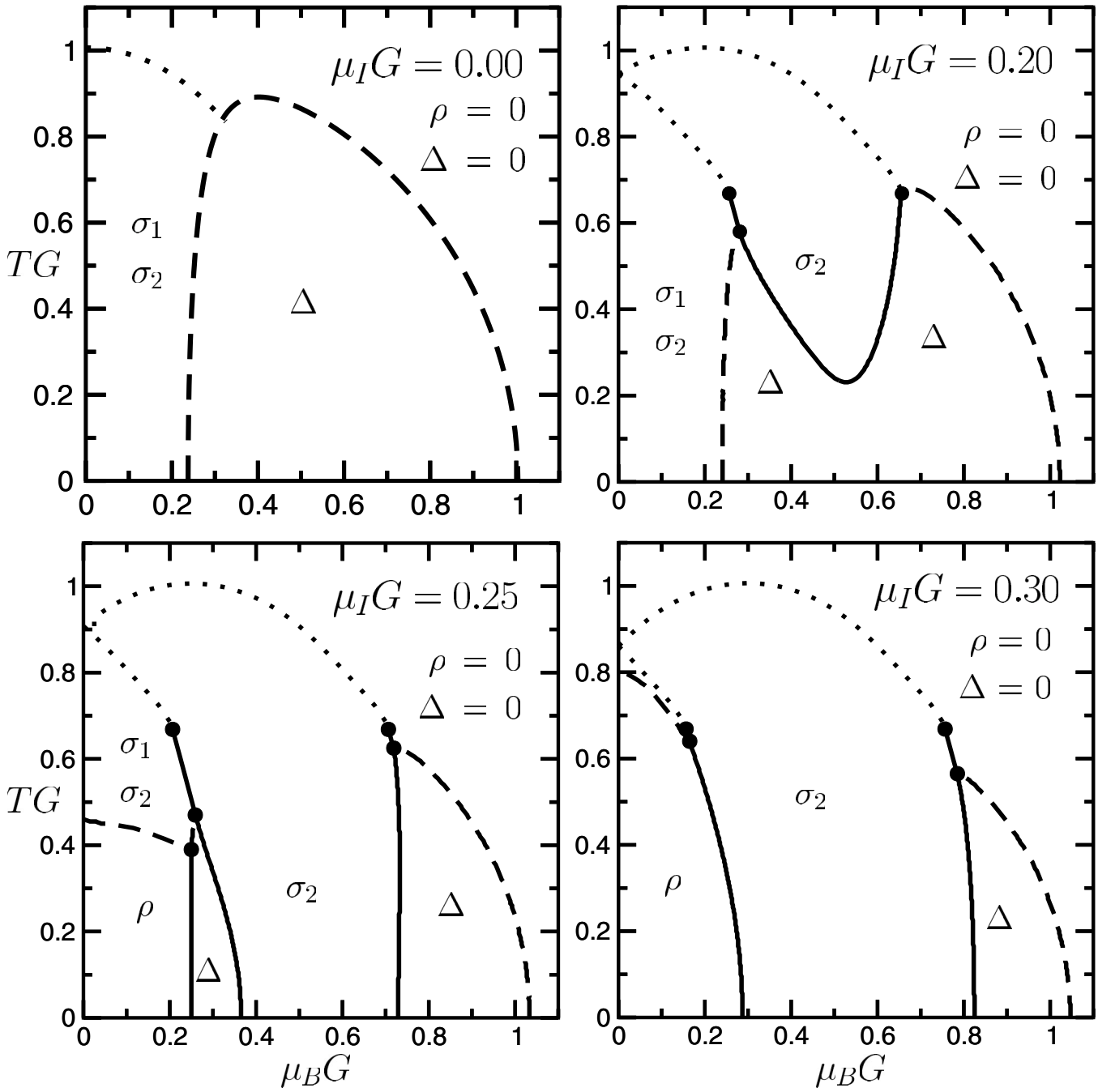

FIG. 6. Phase diagram in the μ_B–T-plane at fixed values of the isospin chemical potential $\mu_I G$ for a finite quark mass of $mG = 0.1$. Values for $\mu_I G$ are given in the panels. First (second) order transitions are indicated by solid (dashed) lines, the dotted lines indicate a crossover. Phases are labeled by the nonvanishing condensates, or the condensates with large expectation values.

two flavors and nonzero baryon chemical potential, isospin chemical potential and temperature. Our temperature term respects the flavor symmetry of the partition function as it should.

The random matrix partition function has been rewritten exactly in terms of an effective Lagrangian. To lowest order in the chiral perturbation expansion, the effective Lagrangian agrees with the one derived in chiral perturbation theory [9,10,13]. We have analyzed the phase diagram of this model for values of the mass and chemical potential outside of the domain of chiral perturbation theory. It shows a rich phase structure with phases characterized by the diquark condensate, the pion condensate and the chiral condensates, $\langle \bar{u}u \rangle$ and $\langle \bar{d}d \rangle$. In the presence of two chemical potentials, the chiral condensates are not necessarily equal. For a nonzero quark mass, in regions without pion or baryonic condensate at small values for the chemical potentials, the restoration of the spontaneously broken sym-

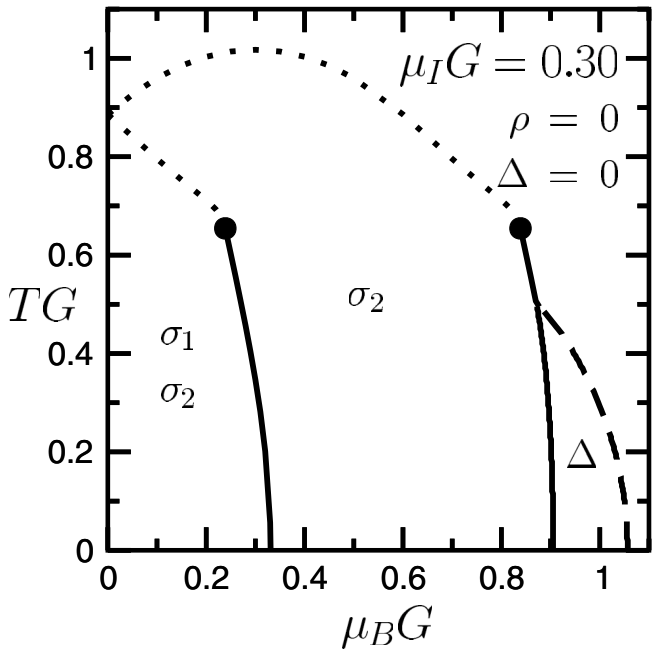

FIG. 7. Phase diagram in the μ_B–T-plane at fixed values of the isospin chemical potential $\mu_I G = 0.3$ for a finite quark mass of $mG = 0.2$. First (second) order transitions are indicated by solid (dashed) lines, the dotted lines indicate a crossover. Phases are labeled by the nonvanishing condensates, or the condensates with large expectation values. This phase diagram is very similar for either QCD with two colors or for QCD with three colors.

metry takes place via two separate crossovers, across which the chiral condensates for the two flavors rapidly change in value. The vanishing of the superfluid phases at large values of the relevant chemical potentials, which is also observed on the lattice, has been explained as a saturation effect. On the lattice, this is due to the finite number of lattice sites [27], and for random matrix models, this is due the compactness of the Dirac operator.

The tricritical point of the diquark and pion condensation transitions observed in lattice calculations [26,28–30] is absent in the random matrix models. Since the Random matrix partition function is equivalent to a mean field description of the phase transition, this is not entirely surprising. Symmetries alone do not determine the presence of a tricritical point. In chiral perturbation theory, a tricritical point is obtained from a one-loop effective potential [12,33]. Ultimately, the question of the structure of the phase diagram in this regard must be answered by lattice calculations [30].

Finally, we would like to compare our results with the random matrix study of the phase diagram for three-color QCD at nonzero temperature, baryon and isospin chemical potentials [34]. First we notice that the upper-left quadrant of the phase diagram in the μ_B–μ_I-plane is identical in both cases. This is due to the fact that in both cases, the isospin chemical potential is related to Goldstone bosons of the microscopic theory. The upper-right quadrants are obviously different in the two theories, since there is no Goldstone boson that carries baryon number in three-color QCD. However, the phase diagram for three-color QCD with three quark flavors of equal masses at nonzero isospin and strange chemical potential should be very similar to the one we have presented here.

Second, and more importantly, we notice that it is possible to find a quark mass and an isospin chemical potential for which the diquark and pion condensation phases appear only in certain regions of the phase diagram. Namely, they are present only at low temperature and either very small or very large values of the baryon chemical potential. As shown in Figs. 6 and 7, we see that the first order transition lines of the chiral transitions and their critical endpoints are not at all affected by the phases with bosonic condensates. Indeed, the transition lines are identical to those that are found in the random matrix model for three-color QCD. This observation implies that the critical endpoint of three-color QCD can be studied in two-color QCD. For an appropriate choice of quark mass and isospin chemical potential, the phase diagram in the μ_B–T-plane are almost identical for QCD with two colors and for QCD with three colors. In particular, the doubling of the critical lines due to a nonzero isospin chemical potential can be studied in QCD with two colors.

ACKNOWLEDGMENTS

J. Kogut, K. Splittorff, and B. Vanderheyden are acknowledged for useful discussions. D. T. is supported in part by the "Holderbank"-Stiftung. This work was partially supported by the U.S. DOE Grant No. DE-FG-88ER40388 and by the NSF under Grant No. NSF-PHY-0102409.

Note added in proof—It was pointed out by Vanderheyden and Jackson [53] that although the temperature term in the random matrix model of [49] and [51] superficially violates flavor symmetry, after a unitary transformation, it is actually equivalent to the temperature term of the random matrix model in the present work.

[1] M. G. Alford, K. Rajagopal, and F. Wilczek, Phys. Lett. B **422**, 247 (1998).

[2] R. Rapp, T. Schäfer, E. V. Shuryak, and M. Velkovsky, Phys. Rev. Lett. **81**, 53 (1998).

[3] A. B. Migdal, O. A. Markin, and I. I. Mishustin, Sov. Phys. JETP **39**, 212 (1974) [Zh. Eksp. Teor. Fiz. **66**, 443 (1974)].

[4] D. T. Son and M. A. Stephanov, Phys. Rev. Lett. **86**, 592 (2001).

[5] A. Barducci, R. Casalbuoni, S. De Curtis, R. Gatto, and G. Pettini, Phys. Lett. B **231**, 463 (1989); Phys. Rev. D **41**, 1610 (1990); A. Barducci, R. Casalbuoni, G. Pettini, and R. Gatto, Phys. Rev. D **49**, 426 (1994).

[6] M. A. Halasz, A. D. Jackson, R. E. Shrock, M. A. Stephanov, and J. J. M. Verbaarschot, Phys. Rev. D **58**, 096007 (1998).

[7] K. Rajagopal and F. Wilczek, *The condensed matter physics of QCD*, in At the Frontier of Particle Physics/ Handbook of QCD, Vol. 3, edited by M. Shifman (World Scientific, Singapore, 2001), p. 2061.

[8] D. T. Son, Phys. Rev. D **59**, 094019 (1999).

[9] J. B. Kogut, M. A. Stephanov, and D. Toublan, Phys. Lett. B **464**, 183 (1999).

[10] J. B. Kogut, M. A. Stephanov, D. Toublan, J. J. M. Verbaarschot, and A. Zhitnitsky, Nucl. Phys. **B582**, 477 (2000).

[11] K. Splittorff, D. Toublan, and J. J. M. Verbaarschot, Nucl. Phys. **B620**, 290 (2002).

[12] K. Splittorff, D. Toublan, and J. J. M. Verbaarschot, Nucl. Phys. **B639**, 524 (2002).

[13] K. Splittorff, D. T. Son, and M. A. Stephanov, Phys. Rev. D **64**, 016003 (2001).

[14] E. Dagotto, F. Karsch, and A. Moreo, Phys. Lett. B **169**, 421 (1986).

[15] E. Dagotto, A. Moreo, and U. Wolff, Phys. Rev. Lett. **57**, 1292 (1986).

[16] E. Dagotto, A. Moreo, and U. Wolff, Phys. Lett. B **186**, 395 (1987).

[17] R. Aloisio, A. Galante, V. Azcoiti, G. Di Carlo, and A. F. Grillo, in *Proceedings of the International Workshop on Non-Perturbative Methods and Lattice QCD, Guangzhou, 2000*, (World Scientific, Singapore, 2001) 123; hep-lat/ 0007018.

[18] R. Aloisio, V. Azcoiti, G. Di Carlo, A. Galante, and A. F. Grillo, Phys. Lett. B **493**, 189 (2000).

[19] R. Aloisio, V. Azcoiti, G. Di Carlo, A. Galante, and A. F. Grillo, Nucl. Phys. **B606**, 322 (2001).

[20] S. Hands, J. B. Kogut, M. P. Lombardo, and S. E. Morrison, Nucl. Phys. **B558**, 327 (1999).

[21] S. Hands, I. Montvay, S. Morrison, M. Oevers, L. Scorzato, and J. Skullerud, Eur. Phys. J. C **17**, 285 (2000).

[22] S. J. Hands, B. Kogut, S. E. Morrison, and D. K. Sinclair, Nucl. Phys. B Proc. Suppl. **94**, 457 (2001).

[23] Y. Liu, O. Miyamura, A. Nakamura, and T. Takaishi, *Proceedings of the International Workshop on Non-Perturbative Methods and Lattice QCD, Guangzhou, 2000* (World Scientific, Singapore, 2001) 132; hep-lat/ 0009009.

[24] S. Muroya, A. Nakamura, and C. Nonaka, nucl-th/ 0111082.

[25] S. Muroya, A. Nakamura, and C. Nonaka, Phys. Lett. B **551**, 305 (2003).

[26] J. B. Kogut, D. Toublan, and D. K. Sinclair, Phys. Lett. B **514**, 77 (2001).

[27] J. B. Kogut, D. K. Sinclair, S. J. Hands, and S. E. Morrison, Phys. Rev. D **64**, 094505 (2001).

[28] J. B. Kogut and D. K. Sinclair, Phys. Rev. D **66**, 014508 (2002).

[29] J. B. Kogut and D. K. Sinclair, Phys. Rev. D **66**, 034505 (2002).

[30] J. B. Kogut, D. Toublan, and D. K. Sinclair, Nucl. Phys. **B642**, 181 (2002).

[31] J. B. Kogut, D. Toublan, and D. K. Sinclair, Phys. Rev. D **68**, 054507 (2003).

[32] Y. Nishida, K. Fukushima, and T. Hatsuda, Phys. Rep. **398**, 281 (2004).

[33] G. V. Dunne and S. M. Nishigaki, Nucl. Phys. **B670**, 307 (2003).

[34] B. Klein, D. Toublan, and J. J. M. Verbaarschot, Phys. Rev. D **68**, 014009 (2003).

[35] D. Toublan and J. B. Kogut, Phys. Lett. B **564**, 212 (2003).

[36] M. Frank, M. Buballa, and M. Oertel, Phys. Lett. B **562**, 221 (2003).

[37] A. Barducci, R. Casalbuoni, G. Pettini, and L. Ravagli, Phys. Rev. D **69**, 096004 (2004).

[38] A. Barducci, G. Pettini, L. Ravagli, and R. Casalbuoni, Phys. Lett. B **564**, 217 (2003).

[39] E. V. Shuryak and J. J. M. Verbaarschot, Nucl. Phys. **A560**, 306 (1993).

[40] J. J. M. Verbaarschot, Phys. Rev. Lett. **72**, 2531 (1994).

[41] J. C. Osborn, D. Toublan, and J. J. Verbaarschot, Nucl. Phys. **B540**, 317 (1999).

[42] P. H. Damgaard, J. C. Osborn, D. Toublan, and J. J. M. Verbaarschot, Nucl. Phys. **B547**, 305 (1999).

[43] D. Toublan and J. J. M. Verbaarschot, Nucl. Phys. **B560**, 259 (1999).

[44] D. Toublan and J. J. M. Verbaarschot, Nucl. Phys. **B603**, 343 (2001).

[45] A. D. Jackson and J. J. M. Verbaarschot, Phys. Rev. D **53**, 7223 (1996).

[46] T. Wettig, H. A. Weidenmueller, and A. Schaefer, Nucl. Phys. **A610**, 492C (1996).

[47] M. A. Stephanov, Phys. Rev. Lett. **76**, 4472 (1996).

[48] D. Toublan and J. J. M. Verbaarschot, Int. J. Mod. Phys. B **15**, 1404 (2001).

[49] B. Vanderheyden and A. D. Jackson, Phys. Rev. D **61**, 076004 (2000).

[50] B. Vanderheyden and A. D. Jackson, Phys. Rev. D **62**, 094010 (2000).

[51] B. Vanderheyden and A. D. Jackson, Phys. Rev. D **64**, 074016 (2001).

[52] B. Vanderheyden and A. D. Jackson, Phys. Rev. D **67**, 085016 (2003).

[53] B. Vanderheyden and A. D. Jackson, Phys. Rev. D **72**, 016003 (2005).